Biosensors and Bioelectronics 24 (2009) 2255–2259

Contents lists available at ScienceDirect

Biosensors and Bioelectronics

journal homepage: www.elsevier.com/locate/bios

Short communication

A novel label-free multi-throughput optical biosensor based on localized surface plasmon resonance

Haowen Huang[a,b,*], Chaocai He[a], Yunlong Zeng[a], Xiaodong Xia[a], Xianyong Yu[a,b], Pinggui Yi[a], Zhong Chen[b]

[a] School of Chemistry and Chemical Engineering, Hunan University of Science and Technology, Xiangtan, China
[b] State Key laboratory of Physical Chemistry of Solid Surface, Xiamen University, Xiamen, China

ARTICLE INFO

Article history:
Received 16 September 2008
Accepted 9 October 2008
Available online 25 October 2008

Keywords:
Localized surface plasmon resonance
Label-free
Gold nanorods
Longitudinal plasmon wavelength

ABSTRACT

A novel and sensitive multi-throughput localized surface plasmon resonance (MLSPR) biosensor was developed for the first time. Various gold nanorods with different aspect ratios were used to fabricate the optical sensor. Five kinds of gold nanorods with different aspect ratios were chosen to construct five throughputs of MLSPR. Various LSPR peaks imply that different acceptor–ligand pairs can be detected simultaneously in the wavelength range from 530 to 940 nm. The biosensor immobilized on glass slides was applied to label-free detection between acceptor and ligand. The MLSPR-based optical biosensor can be used to detect three antigen–antibody pairs simultaneously. The biosensor proposed herein is easy to fabricate, and its operation procedure is convenient as labeling procedure is unnecessary.

1. Introduction

In life sciences, there has been a continuously growing interest to find new methods and devices that would provide easy, highly reproducible, and sensitive sensing assays for biomolecular reactions. Localized surface plasmon resonance (LSPR) based on metal nanoparticles is one of powerful candidates for biotechnology and biosensor (Imura et al., 2004; Endo et al., 2005; Dahlin et al., 2006; Marinakos et al., 2007; Gish et al., 2007; Yu and Irudayaraj, 2007). The optical properties of nanoparticles strongly depend on both size and shape of the nanoparticles. Gold nanorods possess two plasmon bands: one is transverse plasmon wavelength (TPW) and another is longitudinal plasmon wavelength (LPW) appearing in visible or NIR range. These anisotropic gold nanorods have the potential to be utilized as molecular probes since significant changes occur in the plasmon spectra in response to a change in the refractive index in the vicinity of gold nanorods, a perfect property for sensing specific target binding events. El-Sayed and co-workers (Lee and El-Sayed, 2006; Link and El-Sayed, 2005; Nikoobakht and El-Sayed, 2003) have demonstrated that, both experimentally and theoretically, the LPWs are highly sensitive to changes in the dielectric properties of the surroundings and the sensitivity increases as the aspect ratio of the nanorods increases (Jain et al., 2006). Currently, Most of biosensors utilizing LSPR of gold nanoparticles are mainly performed by monitoring plasmon absorption wavelength shift. On the other hand, the biosensor can be performed by monitoring their plasmon absorption intensity changes at a fixed wavelength.

However, when the gold nanoparticles are used in the form of a liquid solution, regardless of their shape and size, the inherent artificial signals from the changes in nanoparticle concentrations cannot be avoided. When multiple washing steps are incorporated to remove unbound analytes, uncertain changes in the nanoparticle concentration may occur and induce the extinction intensity changes, thus making it inaccurate to monitor biospecific interaction events. To solve this problem, one effective strategy is to chemically immobilize the gold nanoparticles on glass surface instead of in suspension. Hence, the concentration of nanoparticles can be kept constant throughout the experimental process (Nath and Chilkoti, 2002, 2004; Chen et al., 2007).

In the past decade, surface plasmon resonance (SPR) biosensor has been developed utilizing the sensitivity of propagating surface plasmon resonance of a thin noble metal layer to the refractive indices of bulk to the thickness of thin films. However, conventional SPR sensors are difficult to be integrated in a large-scale array format. Because LPW of gold nanorods strongly depends on the length-to-diameter aspect ratio of the nanorods (Daniel and Astruc, 2004; Murphy et al., 2005; Térez-Juste et al., 2005), as a result, the corresponding LPW can be fine-tuned by adjusting the length and diameter of nanorods. If varied gold nanorods with different LPW are carefully designed and then assembled on chips, a significant

* Corresponding author at: School of Chemistry and Chemical Engineering, Hunan University of Science and Technology, Xiangtan, China. Tel.: +86 723 8290045; fax: +86 732 8290509.
E-mail address: hhwn@iccas.ac.cn (H. Huang).

0956-5663/$ – see front matter © 2008 Elsevier B.V. All rights reserved.
doi:10.1016/j.bios.2008.10.013

multi-throughput for simultaneous detection of multiple targets could be achieved. Therefore, a new type of multi-throughput optical biosensor can be fabricated based on the tunable LPW of gold nanorods, with the advantages of label-free detection, low cost and broad tunability.

In this work, we demonstrated for the first time a multi-throughput localized surface plasmon resonance (MLSPR) biosensor using gold nanorods immobilized on glass slides. The detection of target binding was performed via direct spectral changes induced by the changes of refractive index in the vicinity of individual particles. In addition to preserving the desirable features of conventional SPR sensors, this sensor is also convenient to be fabricated, and requires only a vis–NIR spectrometer for detection purposes. Even more impressive, the sensor can operate in the NIR region, which usually falls into certain characteristic absorption bands of biomacromolecules. This is very useful for monitoring various acceptor–ligand pairs simultaneously and thus the sensor has the potential to be developed as a high throughput biosensor.

2. Experimental

2.1. Preparation of gold nanorods

Seed solution of gold nanorods was prepared according to the previous methods (Jana et al., 2002; Nikoobakht and El-Sayed, 2003). Cetyltrimethylammonium bromide (CTAB) solution (1.5 mL, 0.1 M) was mixed with 100 μL of 0.02 M $HAuCl_4$. To the stirred solution, 100 μL of ice-cold 0.01 M $NaBH_4$ was added, which resulted in the formation of a brownish yellow solution. Vigorous stirring of the seed solution continued for 2 min. The seed solution was kept at room temperature (25 °C) and was used at least 2 h after its preparation.

To grow gold nanorods, 1.5 mL of 0.02 M $HAuCl_4$ and 1.0 mL of 0.01 M $AgNO_3$ were added into 30 mL of 0.1 M CTAB, followed by the addition of 0.8 mL of 0.08 M ascorbic acid. Ascorbic acid here works as a mild reducing agent and changes the growth solution from dark yellow to colorless. Finally, 70 μL of the seed solution was added to the growth solution. The color of the solution gradually changed within 15 min. By this means, gold nanorods with LPW shorter than 850 nm were generated. Those nanorods with LPW longer than 850 nm were synthesized according to the method introduced in our previous study (Huang et al., 2008a,b).

Prior to immobilization of the gold nanorods on the mercaptoterminated silane SAM on glass, excess CTAB was removed from the suspension of gold nanorods by careful centrifugation at 16,000 rpm for 15 min. In the end, the nanorods were redispersed in 0.005 M CTAB solution via sonication.

2.2. Immobilization of gold nanorods on glass

Glass slides were cleaned by immersion in piranha (caution: piranha is a vigorous oxidant and should be used with extreme caution) solution at 70 °C for 30 min. After cooling to room temperature, the slides were moved out and rinsed repeatedly with water, and then were sonicated for 10 min. Subsequently, the slides were rinsed repeatedly with ethanol and were then incubated in a 3-mercapto-propyl-trimethoxy-silane (MPTMS) 5% ethanol solution for 4 h. The slides were followed by being rinsed with ethanol and deionized water in sequence, and air-dried at room temperature before further modification. Finally, the mercaptosilane-modified glass slides were incubated in the suspension for 30 min to prepare the gold nanorod chips. These chips were measured with a vis–NIR spectrophotometer.

2.3. Surface attachment chemistry

Mercaptoundecanoic acid (MUA) monolayers were formed on gold nanorods films by immersing the glass slides immobilized with nanorods into a 5 mM ethanol solution for at least 18 h, followed by thorough rinsing with ethanol and water. The modified nanorods films were bonded to *N*-hydroxysuccinimide (NHS) by being immersed in aqueous solution of 75 mM *N*-ethyl-*N*-[(dimethylamino) propyl]carbodiimide (EDC) and 15 mM NHS for 30 min. To attach biological macromolecules on the surface, the glass slides with NHS-terminated nanorods were incubated in human IgG (titers of IgG antibody equal to 16), goat IgG (titers of IgG antibody equal to 16), and rabbit IgG (titers of IgG antibody equal to 16) solution (0.01 g/L), respectively. After reaction for about 30 min, the glass slides were rinsed with phosphate buffer saline (PBS) and then blocked by 1 M ethanolamine (pH 8.5) for 10 min. In the end, the unreactive ethanolamine was removed and the glass slides were rinsed exhaustively with water.

2.4. Experimental setup of multi-throughput LSPR

The scheme of MLSPR and the digital picture of the MLSPR experimental setup are shown in Fig. 1, where glass slides immobilized with gold nanorods act as sensor chips. This setup is easy to fabricate, and requires only a UV–vis spectrometer (Lambda 35, PerkinElmer, US) for detection purposes. A specially modified cuvette is fabricated for the flow injection of the samples. The detecting glass slides are inserted into the cuvette, where the glass slides are specially designed in order to arrange as more sensor chips as possible separately in the cuvette. All absorption spectra were taken from 400 to 1100 nm on the UV–vis spectrophotometer at room temperature.

3. Results and discussion

3.1. Fabrication of multi-throughput LSPR

For an ideal MLSPR biosensor, the immobilized gold nanorods should be able to display LSPR peaks in a wide range, with the neighboring LPWs being distinctly separated. Therefore, it is crucial to choose appropriate gold nanorods. As is known, each kind of gold nanorods has their intrinsic LSPR wavelength and corresponding peak width, but only those showing small peak widths can achieve qualified peak resolution essential for construction of MLSPR sensors that are capable of detecting acceptor–ligand pairs within certain wavelength range. Since small peak widths of nanorods are resulted from a narrow distribution of their shape and size, the preparation of gold nanorods should concentrate on particle size consistency. Gold nanorods of various aspect ratios, which display accurate LPWs, can be obtained according to the methods developed in our previous study (Huang et al., 2008a,b). TEM images of these gold nanorods are also shown in Supplemental information (Fig. 4). Fig. 2A shows the spectra that display the corresponding LSPR peaks of five kinds of nanorods, and Fig. 2B exhibits the MLSPR spectrum comprising the five kinds of nanorods immobilized on glass slides. It can be clearly seen that these LPWs are distinguished from each other, implying a potential for multi-throughput detection and possibility of the fabricated sensor chip to detect five acceptor–ligand pairs simultaneously. Akin to conventional SPR, LSPR can detect biological macromolecules by measuring their refractive index changes caused by even slight molecular structure fluctuations. While the first peak TPW, the plasmon peak near 520 nm, is not sensitive enough to perceive the refractive index changes induced by specific target binding, the longitudinal peaks of the nanorods (>520 nm) are excellent reporters of such events

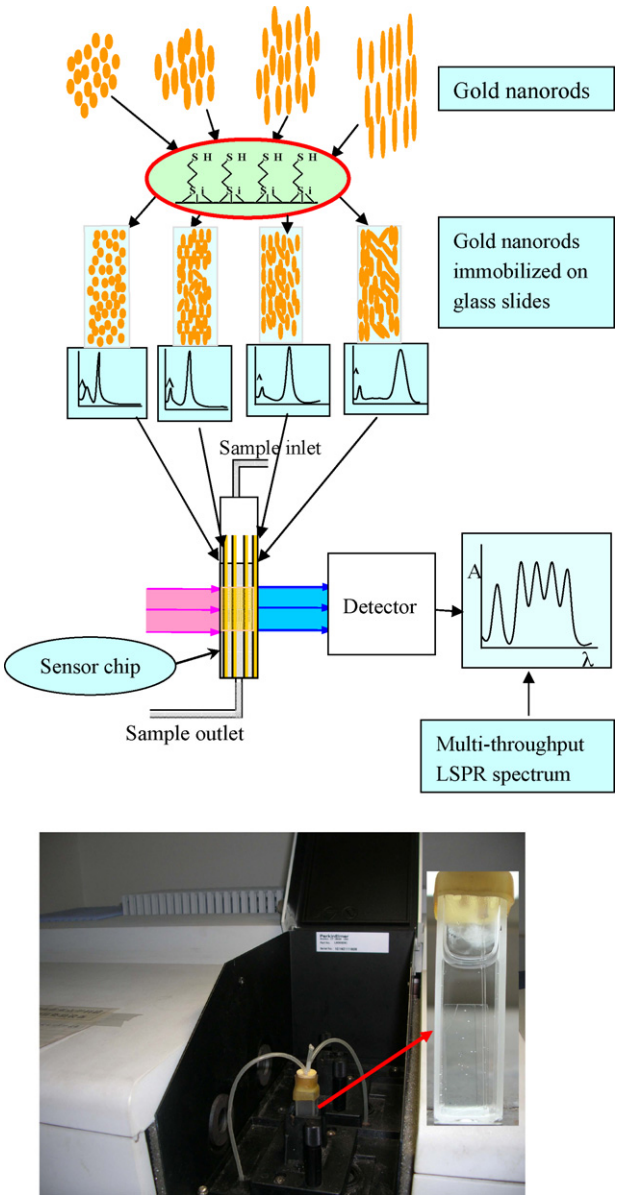

Fig. 1. Scheme of multi-throughput localized surface plasmon resonance (MLSPR) (top) and the digital picture of real MLSPR setup (bottom).

(Miller and Lazarides, 2005). Generally, for regular LSPR apparatus, the gold nanorods are furnished in the cuvette mounted vertically on an optical bench, and the transmission light is detected by a single-element detector. In the same way, MLSPR can measure the change in transmission across the sample, which the specifically designed sensor chips insert in the detection cell. As illustrated in Fig. 1, a closed flow cell was assembled consisting of several separate glass slides coated with nanorods modified with biomolecules. There are two pipes to connect the input and output flows. This flow cell was mounted vertically on an optical bench between the light source and the transducer. A pump controls the flow rate. Therefore no special detector is needed in the fabricated MLSPR sensor. More importantly, multiplex points associated with various acceptor–ligand pairs can be measured simultaneously. Besides all of these advantages, the MLSPR setup in this study can also undergo a real-time monitoring of the interactions between acceptors and ligands, preserving the desirable features of conventional SPR sensors suitable for kinetic study.

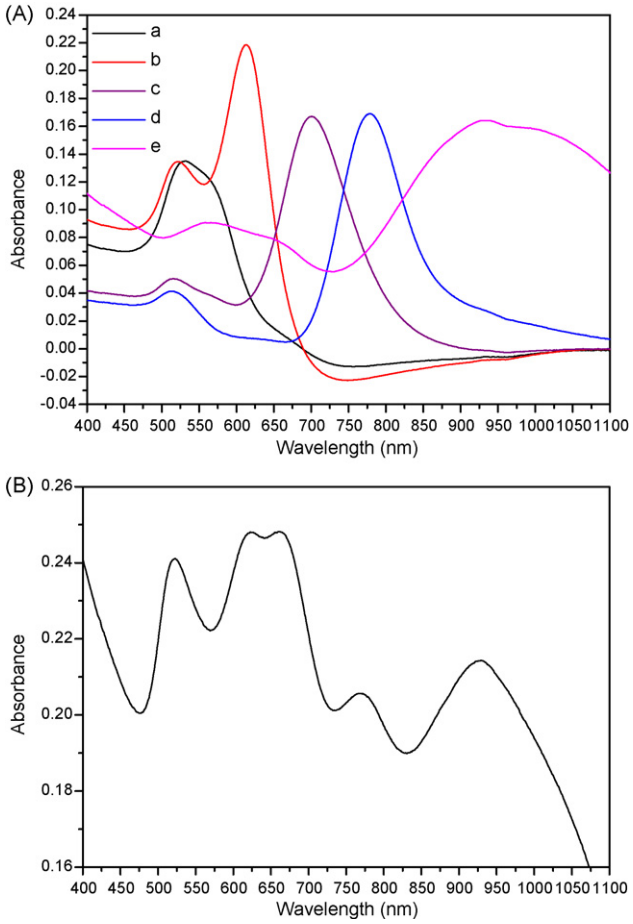

Fig. 2. (A) Absorption spectra of gold nanorods with five kinds of LPWs (a: 532 nm, b: 613 nm, c: 700 nm, d: 779 nm, and e: 935 nm). (B) MLSPR spectrum comprises five LSPR peaks resulted from gold nanorods related to (A).

3.2. Detection of biological targets using MLSPR

For gold nanorods, the aspect ratio dependence of LPW inherently provides the potential of multiplex data points collection. To the best of our knowledge, heretofore this advantage has not been fully utilized. In this work, we managed to accomplish multiplex detection of various targets by constructing a system comprising two and three gold nanorods target pairs. The utility of the gold nanorod chip as biomolecular sensor was investigated through using a model receptor–analyte system, MUA-IgG. Briefly, immobilized nanorods were modified with self-assembled monolayer (SAM) of MUA. An amine-terminated IgG was coupled to the carboxylic acid groups presented by MUA via EDC/NHS activation, and the ethanolamine was incorporated into the SAM to reduce nonspecific binding.

Human IgG and goat IgG were coupled to the SAM to serve as capture antibodies, so that the binding of specific and nonspecific antibodies could be studied. The absorption peaks of the gold nanorods immobilized on glass slides were observed at 687 and 939 nm, respectively. A red-shift about 25 nm was observed when the nanorods corresponding to LPW 939 nm were linked to human IgG, as shown in Supplemental information (Fig. 5). Similarly, a significant red-shift of LPW about 20 nm was found when goat IgG interacted with other nanorods, finally, this peak centered at 707 nm (not shown here). These distinct evidences show that the two kinds of IgG were successfully bound on the surface of nanorods.

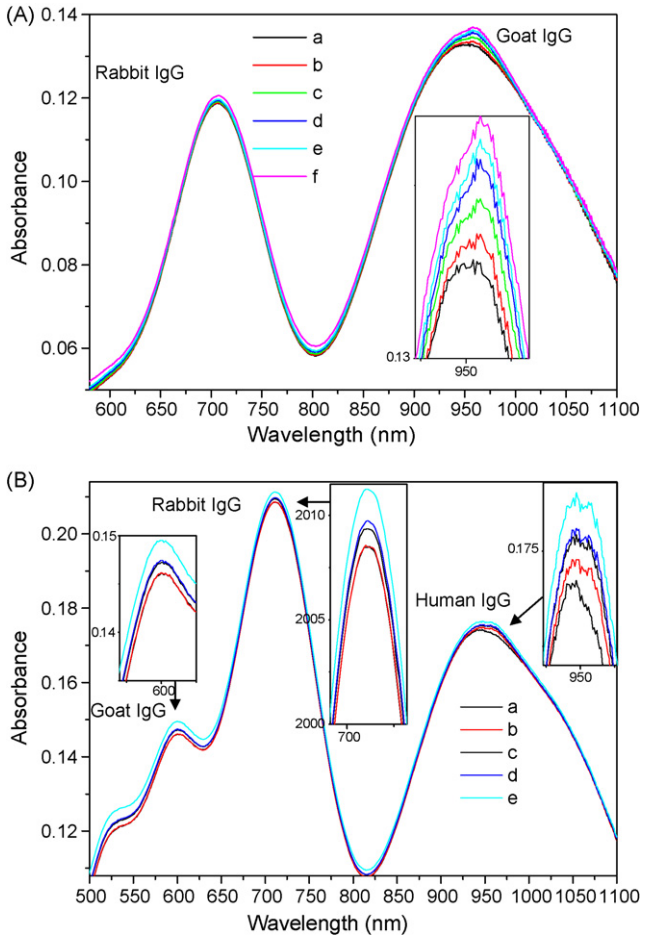

Fig. 3. (A) MLSPR spectra acquired by the addition of rabbit anti-goat IgG. Curve a represents two different gold nanorods linked with goat IgG and rabbit IgG, respectively; b–f represent gradual increasing concentration of rabbit anti-goat IgG (1:2400, 1:1200, 1:800, 1:600, and 1:480). (B) MLSPR spectra acquired by the addition of various anti IgGs. Curve a consists of three LSPR peaks related with various gold nanorods immobilized with goat IgG, rabbit IgG and human IgG, respectively; b represents diluted 1:1200 times rabbit anti-human IgG, c and d represent diluted 1:1200 and 1:800 times goat anti-rabbit IgG, respectively, and e represents 1:240 times rabbit anti-goat IgG.

The optical characteristic evaluation of anti-IgG was carried out using the IgG probe immobilized on LSPR-based optical biosensors. Firstly, the MLSPR biosensor chips were immersed in PBS solution, and the absorption spectra of LSPR were recorded. Subsequently samples containing anti-IgG were added. Then, a gradual increase of peak intensity occurred. However, instead of obvious wavelength shift, a significant increase in the absorbance intensity was observed. The LSPR peak wavelength throughout such reactions is displayed in Fig. 3A. As can be seen from this figure, the intensity of LSPR peak varies with rabbit anti-goat IgG flowing through two-throughput MLSPR. This indicated that the rabbit anti-goat IgG reacted specifically with the goat IgG immobilized on gold nanorods at lower concentration. Like other polyclonal antibodies, the detection of polyclonal rabbit anti-goat IgG by immunological methods is often hampered by the cross-reactivity. Higher concentration of rabbit anti-goat IgG will lead to the cross-reactivity, and peak intensity corresponding to rabbit IgG was found to increase when the concentration of rabbit anti-goat IgG increased up to 1:800 (serum of rabbit anti-goat IgG: PBS = 1:800) in the experiment. In this study, 1:2400 rabbit anti-goat IgG can be detected. There is a good linear relationship between the absorption intensity of goat IgG and the concentrations of rabbit anti-goat IgG in our experiment (shown in Supplemental information Fig. 6).

Fig. 3B illustrates the evolution of MLSPR spectra acquired by the addition of various anti IgGs. Firstly, an increase of intensity corresponding to LPW 939 nm was observed via the addition of rabbit anti-human IgG maintaining concentration at 1:1200, whereas no increase of intensity was observed for other two peaks, suggesting the rabbit anti-human IgG reacted specifically with human IgG immobilized on the gold nanorods. Secondly, the addition of goat anti-rabbit IgG of lower concentration led to an increase of the LSPR peak related to the immobilized rabbit IgG. 1:1200 goat anti-rabbit IgG can be detected readily. Thirdly, 1:1200 rabbit anti-goat IgG can be detected through the increase of LSPR peak intensity related to goat IgG. The peak intensity linearly increases with the concentration of rabbit anti-goat IgG, and detectable changes occurred in other two peaks with the rabbit anti-goat IgG increasing up to 1:600, which suffered from the cross-reactivity of ploYclonal antibodies. It is reasonable to believe that it can extend detection range and throughput of this biosensor if more highly specific acceptor–ligand systems are investigated.

Separate experiment was conducted to investigate the effect on cross-reactivity among the polyclonal anti IgGs. The gold nanorods immobilized on glass slide modified with rabbit IgG were placed into a cuvette furnished with PBS solution and the LSPR peak was observed at 684 nm. A sample of rabbit anti-goat IgG was firstly added, and no significant increase of the LSPR peak intensity was observed at lower concentration. However, with the concentration of rabbit anti-goat IgG increasing up to 1:600, a small change of the intensity of the LSPR peak appeared (shown in Supplemental information Fig. 7). Then the sample of goat anti-rabbit IgG instead of rabbit anti-goat IgG was added, and a gradual increase of peak intensity occurred. Finally, the addition of goat anti-rabbit IgG was stopped and another sample of rabbit anti-human IgG was continuously added. No distinct change of the intensity was found until the concentration increasing up to 1:600.

4. Conclusions

In this communication, we demonstrated for the first time that the exquisite optical properties of gold nanorods could be utilized to develop simple and sensitive biosensors for multi-throughput detection of biological targets. The MLSPR-based optical biosensor constructed with gold nanorods immobilized on glass slides was applied to the detection of the reaction between antigens and antibodies, which is label-free, cost-effective and easy to fabricate. More importantly, this biosensor can simultaneously detect various acceptor–ligand pairs through choosing proper gold nanorods with various aspect ratios in a wide wavelength range, manifesting its potential to be developed into a high throughput detection device. The concept and methodology depicted in this study can serve as the basis for developing new multi-throughput assays to detect molecular binding events in medical and life sciences.

Acknowledgements

This work was supported by Scientific Research Fund of Hunan Provincial Education Department (06B028), Key Project of Health and Science and Technology of Xiamen (3502Z20051027), and National Natural Science Foundation of China (20803020, 20772027 and 20423002).

Appendix A. Supplementary data

Supplementary data associated with this article can be found, in the online version, at doi:10.1016/j.bios.2008.10.013.

References

Chen, C.D., Cheng, S.F., Chau, L.K., Wang, C.R.C., 2007. Biosens. Bioelectron. 22, 926–932.
Dahlin, A.B., Tegenfeldt, J.O., Höök, F., 2006. Anal. Chem. 78, 4416–4423.
Daniel, M.C., Astruc, D., 2004. Chem. Rev. 104, 293–346.
Endo, T., Kerman, K., Nagatani, N., Takamura, Y., Tamiya, E., 2005. Anal. Chem. 77, 6976–6984.
Gish, D.A., Nsiah, F., McDermott, M.T., Brett, M.J., 2007. Anal. Chem. 79, 4228–4232.
Huang, H., He, C., Zeng, Y., Xia, X., Yu, X., 2008a. Colloid Surf. A 317, 56–61.
Huang, H., He, C., Zeng, Y., Xia, X., Yu, X., Yi, P., 2008b. J. Colloid Interface Sci. 322, 136–142.
Imura, K., Nagahara, T., Okamoto, H., 2004. J. Phys. Chem. B 108, 16344–16347.
Jain, P.K., Eustis, S., El-Sayed, M.A., 2006. J. Phys. Chem. B 110, 18243–18253.
Jana, N.R., Gearheart, L., Obare, S.O., Murphy, C.J., 2002. Langmuir 18, 922–927.
Lee, K.S., El-Sayed, M.A., 2006. J. Phys. Chem. B 110, 19220–19225.
Link, S., El-Sayed, M.A., 2005. J. Phys. Chem. B 109, 10531–10532.
Marinakos, S.M., Chen, S., Chilkoti, A., 2007. Anal. Chem. 79, 5278–5283.
Miller, M.M., Lazarides, A.A., 2005. J. Phys. Chem. B 109, 21556–21565.
Murphy, C.J., Sau, T.K., Gole, A.M., Orendorff, C.J., Gao, J., Gou, L., Hunyadi, S.E., Li, T., 2005. J. Phys. Chem B109, 13857–13870.
Nath, N., Chilkoti, A., 2002. Anal. Chem. 74, 504–509.
Nath, N., Chilkoti, A., 2004. Anal. Chem. 76, 5370–5378.
Nikoobakht, B., El-Sayed, M.A., 2003. Chem. Mater. 15, 1957–1962.
Térez-Juste, J., Pastoriza-Santos, I., Liz-Marzán, L.M., Vaney, P., 2005. Coordin. Chem. Rev. 249, 1870–1901.
Yu, C., Irudayaraj, J., 2007. Anal. Chem. 79, 572–579.